

A New Multi-Output DC-DC Converter for Electric Vehicle Application

M.Uday Kiran¹, Shaik Arif²

¹Associate Professor, Assistant Professor² Department of Electrical and Electronics Engineering

^{1,2}R K College of Engineering, Vijayawada, India

¹udaymogadati18@gmail.com²arif217shaik@gmail.com

Abstract – Multiport converters play a significant role in portable electronic and electric vehicle (EV) applications. In literature, different configurations of single-input multi-output (SIMO) converters are presented. Most of the SIMO converters generate the outputs with operating constraints on the duty ratio and charging of inductors. The cross regulation problem is still a challenge in SIMO converters design. A SIMO topology is proposed in this study to overcome the limitations mentioned earlier. It can generate three different output voltages without constraint on the duty cycle and inductor currents (like $i_{L1} > i_{L2} > i_{L3}$ or $i_{L1} < i_{L2} < i_{L3}$). Cross regulation problems do not exist in the proposed topology, so the load voltage V_{01} (V_{02}) (V_{03}) is not affected by the variation of output current i_{03} (i_{02}) (i_{01}). The loads are isolated from each other during control. In the laboratory, a 200W proto type circuit is developed; simulation and experimental results are validated.

INDEX TERMS Multiport converters, single input multi output converters.

I. INTRODUCTION

In the past decade, there has been an increase in demand for renewable energy sources utilization in electric vehicles (EVs), auxiliary power, and grid-connected applications [1]–[5]. In the applications, multi port DC-DC converters are essential for Hybridizing energy sources which lead to, reduce the components count, complexity, and cost of the system compared to several separate single input DC-DC converters [6], [7]. Over the past decade, MPC converters have been presented. A new SIMO converter is proposed in [8]. This structure simultaneously generates boost, buck, and inverted outputs controlled in dependently. However, producing 'n' voltage levels requires $n + 2$ switches, which increases the overall size and cost of the converter. Unexpected mistakes in calculating state-space equations and output voltages for a SIMO converter given in [8] are addressed and rectified in [9]. The single coupled inductor-based SIMO buck is presented in [10] with lesser output inductor current ripple than single inductor SIMO converters. Nayak and Nath [11] elaborately presented the comparative performance of SIDO converters based on the coupled inductor and single inductor (SI) in terms of cross-coupling issues. Furthermore, they proposed that the coupled inductor SIDO converter has a better steady-state and transient performance. Nevertheless, in a SISIMO configuration inductor is switched between the loads, which causes high ripples and cross-regulation problems.

II. Proposed simo Configuration and Modes of Operation

The proposed single input three-output DC-DC configurations depicted in Figure 2(a). In this configuration the components are as follows, input voltage V_{DC} , switches (S_1 - S_3), diodes (D_1 - D_3), and passive elements (L_1 - C_1 , L_2 - C_2 , and L_3 - C_3). It can generate three different output voltages, i.e., boost (V_{01}), buck-boost (V_{02}) with positive voltage polarity, and buck (V_{03}). The proposed converter is suitable

for independently regulating the output voltages by the duty cycles D_1 , D_2 and D_3 , respectively. The theoretical waveforms of circuit elements are depicted in Figure 2(b).

The proposed configuration is different from the conventional parallel combination of buck, boost, and buck-boost configuration. In the proposed circuit configuration, the loads are isolated during the simultaneous control. From the following figures, one may observe that during mode-1 operation, load R_3 alone through S_3 is connected to the input powers up- ply, but the other load s are isolated ,as shown in Figure 3(a). Similarly, during mode-2 only load R_1 alone through D_1 is connected to the input supply, but other loads are isolated, as depicted in Figure 3(b). In the proposed control strategy, all the loads are isolated from each other during their control in any mode of operation.

2.1 mode of operation switching state 1

Switches S_1 , S_2 , and S_3 are turned ON. The current flow path is depicted in Figure 3(a), and the energy port V_{DC} magnetizes L_1, L_2 , and L_3 . Consequently, the C_1 and C_2 are discharged to the loads (R_1) and (R_2), respectively, whereas (C_3) is charged. The inductor currents and capacitor voltages are represented in Eq. (1)

switching state 2

It is observed that during switching state-1 operation, load (R_3) alone through S_4 is connected to the ground but the other loads are isolated even when the ground is involved during charging the battery, as shown in Figure 3(a). Similarly, during switching state-2 only load (R_1) alone through D_1 is connected to the ground, but other loads are isolated from the ground and the load (R_1) as well as depicted in Figure 3(b). In the proposed control strategy, all the loads are isolated from each other during their control during any mode of operation. Moreover, the configuration of the circuit is such that energy stored in the inductor is confined to one output only and is not shared with the other outputs during the control and also, which allows controlling the output voltages with independent duty-cycles. As a result, the load voltage V_{01} (V_{02}) (V_{03}) is not influenced by the variation of load current i_{03} (i_{02}) (i_{01}). Hence the proposed configuration with this control approach avoids all the issues about cross- regulation problems even when the ground is involved during battery charging. More importantly, the configuration is simple and it can generate three independent outputs without any assumptions on inductor currents ($i_{L1} > i_{L2} > i_{L3}$ or $i_{L1} < i_{L2} < i_{L3}$ or $i_{L1} = i_{L2} = i_{L3}$) and/or operating duty cycle.

III. SMALL SIGNAL MODELLING

The transfer function of the proposed topology is derived from small signal analysis as [26]. The state-space equations (16)-(25) are as follows

$$[A]X(t) = Bx(t) + Cu(t) \quad (16)$$

$$y(t) = Dx(t) + Eu(t) \quad (17)$$

where state-space coefficients are A, B, C, D and E . $X(t)$ = state vector, $U(t)$ = input vector, and $y(t)$ = output vector. Where, State vector = $x(t)$, Input vector = $u(t)$ and Output vector = $y(t)$. (18)–(21), as shown at the bottom of the next page.

The output voltages V_{01} , V_{02} and V_{03} are determined by d^1 and d^2 , and d^3 Frequency (rad/s)

$$\hat{v}_{01}(s) = G_{vd1} d^1(s), \hat{v}_{02}(s) = G_{vd2} d^2(s),$$

(a)

$$\hat{v}_{03}(s) = G_{vd3} d^3(s) \quad (22)$$

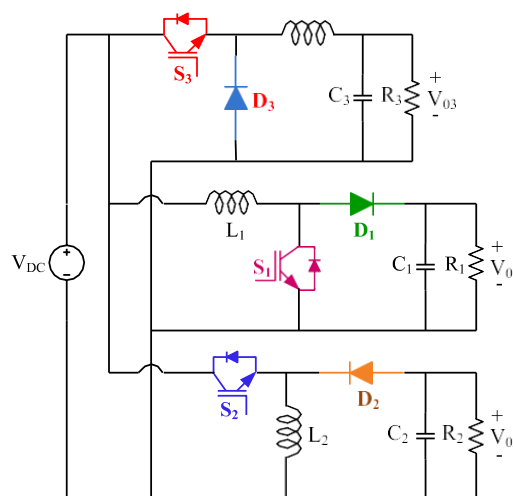
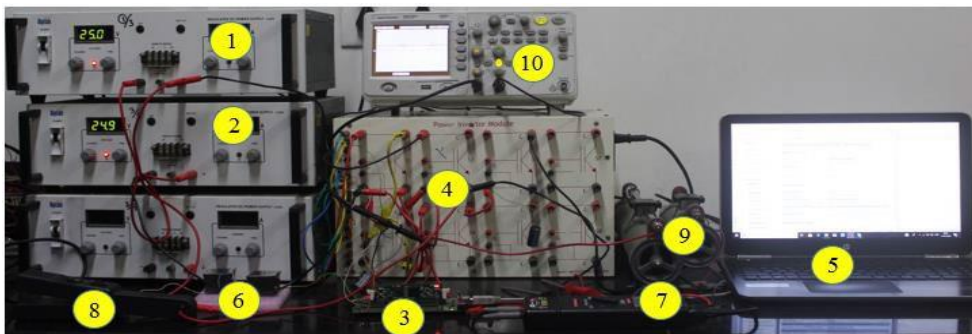
The proposed configuration control transfer function is given in Eq. (23-25) as follows

The bode plot of the proposed configuration is illustrated in Figure 4 for verifying the stability. It is observed that the gain margin is 6.65 dB, 1.54 dB, and -1.55 dB, whereas the phase margin is 90° and 90° and 0.393° respectively

IV. Controller Design, Parameter design, Small-Signal Modeling, Power Losses Calculations, And Comparative Assessment.

A suitable control scheme is essential for good voltage regulation. A control transfer function has been derived for each output by using small-signal modeling. It is cascaded with a controller, as illustrated in Figure 5, where the PI-controller is chosen as given to reduce the un-damped behavior of the system and improve the low-frequency performance i.e., it reduces the steady-state error

V. CIRCUIT DIAGRAM



V. RESULTS AND DISCUSSIONS

Ref.	G_{part}	$S_{V_Stress}/S_{L_Stress}$	$D_{V_Stress}/D_{V_Stress}$	N_S	N_D	N_L	N_C	N_{comp}	N_{input}	N_{output}	Loads are isolated from each other during control
[1]	$D = \frac{V_{01}}{(1-D)}$ $V_{02} = \frac{1}{(1-D)}$ $D < 1$	$V_{Smax} = V_{02}$ $i_{Smax} = i_{L1}$	$V_{Dmax} = V_g - V_{01}$ $i_{Dmax} = i_{L2}$	1	2	2	3	8	1	2	Yes
[1]	$\frac{V_{01}}{(1-D_2)}$ $\frac{V_{02}}{(1-D_2)}$ $D_2 < D_1$	$V_{Smax} = V_{01}$ $I_{Smax} = I_{in}$	$V_{Dmax} = V_{01}$ $I_{Dmax} = I_{01}$	3	2	3	10	1	2	Yes	
[1]	$V_{01} = D_1 V_i, V_{02} = D_2 V_i$ $D_1 + D_2 < 1$	$V_{Smax} = V_i$ $V_{S0-2} = V_i$ $i_{Smax} = i_{L1} + i_{L2}$		3	2	2	7	1	2	Yes	
[2]	$\frac{V_{01} D}{(1-D)}$ $V_{02} = \frac{-V_{in} D}{(1-D)}$ $0 < D < 1$	$V_{Smax} = V_{in} - V_{02}$ $i_{Smax} = i_{L1} + i_L$	$V_{Dmax} = V_{in} + V_{02}$ $V_{Dmax} = V_{01} - V_{02}$	3	2	3	10	1	2	Yes	
[2]	$\frac{V_{01}}{(2-d_1-d_2)}$ $\frac{V_{02}}{(2-d_1-d_2)}$	$V_{Smax} = \frac{V_{01}}{2}$ $i_{Smax} = i_{L1}$		6	2	3	11	1	2	Yes	

- [4] X. Lu, K. L. V. Iyer, C. Lai, K. Mukherjee, and N.C.Kar, “Design and testing of a multi-port sustainable DC fast-charging system for electric vehicles,” *Electr. Power Compon. Syst.*, vol. 44, no. 14, pp.1576–1587, Aug.2016.
- [5] E. Babaei and O. Abbasi, “A new topology for bidirectional multi-inputmulti-output buck direct current–direct current converter,” *Int. Trans.Electr. Energ. Syst.*, vol. 27, no. 2, pp. 1–15, Feb. 2017.
- [6] Z. Rehman, I. Al-Bahadly, and S. Mukhopadhyay, “Multiinput DC–DCconvertersinrenewableenergyapplications—Anoverview,”*Renew.Sus-tain. Energy Rev.*, vol. 41, pp. 521–539, Jan. 2015.
- [7] G.Chen,Y.Liu,X.Qing,andF.Wang,“Synthesisofintegratedmulti-portDC–DC converters with reduced switches,” *IEEE Trans. Ind. Electron.*,vol. 67, no. 6, pp. 4536–4546, Jun. 2019.
- [8] P. Patra, A. Patra, and N. Misra, “A single-inductor multiple-output switcher with simultaneous buck, boost, and inverted outputs,” *IEEETrans. Power Electron.*, vol. 27, no. 4, pp. 1936–1951, Apr. 2012.
- [9] M. Abbasi, A. Afifi, and M.R.A.Pahlavani, “Comments on ‘a single-inductor multiple-output switcher with simultaneous buck, boost, andinvertedoutputs,’”*IEEETrans.PowerElectron.*,vol.34,no.2, pp.1980–1984, Feb.2019.